JACS
JOURNAL OF THE AMERICAN CHEMICAL SOCIETY
Article
Cite This: J. Am. Chem. Soc. XXXX, XXX, XXX−XXX
pubs.acs.org/JACS

Stereodivergent Rhodium(III)-Catalyzed cis-Cyclopropanation Enabled by Multivariate Optimization

Tiffany Piou,[†,§] Fedor Romanov-Michailidis,[†,§] Melissa A. Ashley,[†,⊥] Maria Romanova-Michaelides,[‡,⊥] and Tomislav Rovis*[,†]

[†]Department of Chemistry, Columbia University, New York, New York, United States 10027
[‡]Department of Biochemistry, University of Geneva, 1211 Geneva 4, Switzerland

Supporting Information

ABSTRACT: The design of stereodivergent transformations is of great interest to the synthetic community as it allows funneling of a given reaction pathway toward one stereochemical outcome or another by only minor adjustments of the reaction setup. Herein, we present a physical organic approach to invert the sense of induction in diastereoselective cyclopropanation of alkenes with *N*-enoxyphthalimides through rhodium(III) catalysis. Careful parametrization of catalyst−substrate molecular determinants allowed us to interrogate linear-free energy relationships and establish an intuitive and robust statistical model that correlates an extensive number of data points in high accuracy. Our multivariate correlations-steered mechanistic investigation culminated with a robust and general diastereodivergent cyclopropanation tool where the switch from *trans*- to *cis*-diastereoinduction is attributed to a mechanistic dichotomy. Selectivity might be determined by the flexibility of rhodacyclic intermediates derived from ring-opened versus -unopened phthalimides, induced by both their respective ring size and the Sterimol $\mathbf{B}_1$ parameter of the Cp^X ligand on rhodium.

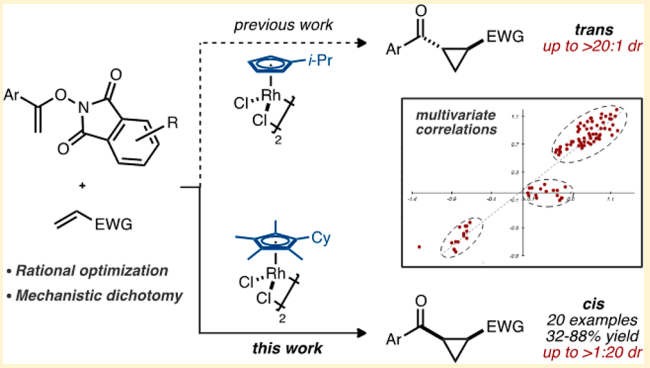

INTRODUCTION

From the perspective of reaction development and process efficiency, modulating the stereoselectivity outcome of synthetic transformations by fine-tuning of the physicochemical properties of the catalyst is highly desirable. Achieving stereodivergency of a given reaction is a daunting task and is typically the result of *ad hoc* adjustments of substrate or catalyst structure, and/or reaction conditions. Hence, strategies developed to this end cannot readily be applied to the design of other stereodivergent reactions.[1] Traditionally, substrate modifications have been widely utilized to drive the reaction to the desired stereochemical pathway, but their applications tend to be limited to specifically engineered precursors.[2−4] In this context, catalyst design is more challenging but ideal for developing versatile transformations.[5−8] Thus, broadly applicable transformations that display catalyst-controllable stereodivergency are in much demand, particularly as a means to accelerate the screening process and structure−activity relationship studies in drug discovery.[9,10]

In the context of our program in rhodium(III) catalysis of C−H activation,[11,12] we have recently discovered an unexpected cyclopropanation reaction of electron-deficient alkenes using *N*-enoxyphthalimides (Scheme 1).[13] Key to achieving high *trans*-stereoselectivity is the design of the η^5-cyclopentadienyl ligand (Cp^X) on rhodium. For example, the prototypical pentamethylcyclopentadienylrhodium(III) catalyst (Cp*Rh(III)) delivers the cyclopropane in a modest 2:1 ratio favoring the *trans*-diastereoisomer. On the other hand, the use of a previously unreported monoisopropyl cyclopentadienyl ligand ($Cp^{i\text{-}Pr}$) allows highly *trans*-diastereoselective cyclopropanation of activated alkenes.[13] Cyclopropanes are reasonably common in natural products,[14−16] but their stereoselective synthesis remains challenging. Although the

Scheme 1. Diastereodivergent Rh(III)-Catalyzed Cyclopropanation Enabled by C−H Bond Activation

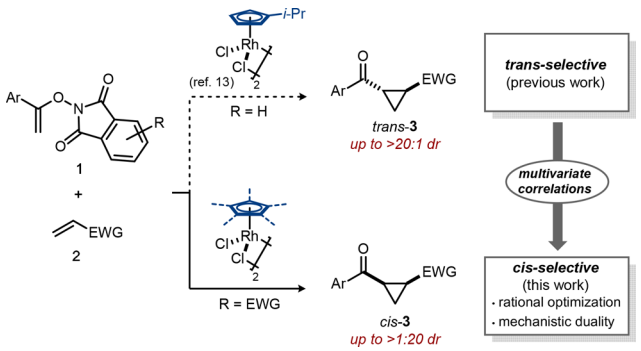

Received: May 7, 2018

DOI: 10.1021/jacs.8b04243
J. Am. Chem. Soc. XXXX, XXX, XXX−XXX

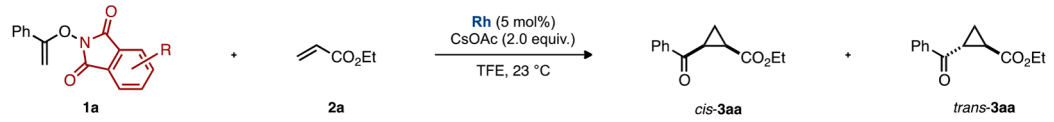

A *with R = H (**1Aa**):*

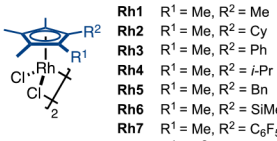

Rh1 R^1 = Me, R^2 = Me
Rh2 R^1 = Me, R^2 = Cy
Rh3 R^1 = Me, R^2 = Ph
Rh4 R^1 = Me, R^2 = *i*-Pr
Rh5 R^1 = Me, R^2 = Bn
Rh6 R^1 = Me, R^2 = $SiMe_3$
Rh7 R^1 = Me, R^2 = C_6F_5
Rh8 R^1 = R^2 = Ph
Rh9 R^1 = Me, R^2 = H
Rh13 R^1 = Me, R^2 = (4-MeO)C_6H_4
Rh14 R^1 = Me, R^2 = (3,5-CF_3)C_6H_3
Rh15 R^1 = Me, R^2 = *t*-Bu

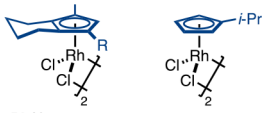

Rh10 R = *t*-Bu
Rh11 R = H
Rh12

entry[a]	Rh	% yield **3aa**[b]	*cis*/*trans* dr[c]
1	**Rh1**	69	34 : 66
2	**Rh2**	60	61 : 39
3	**Rh3**	37	51 : 49
4	**Rh4**	46	46 : 54
5	**Rh5**	55	46 : 54
6	**Rh6**	49	50 : 50
7	**Rh7**	52	62 : 38
8	**Rh8**	*59*	*64 : 36*
9	**Rh9**	58	25 : 75
10	**Rh10**	51	19 : 81
11	**Rh11**	75	9 : 91
12	**Rh12**	77	9 : 91
13	**Rh13**	61	58 : 42
14	**Rh14**	63	61 : 39
15	**Rh15**	30	65 : 35

[a] Conditions: **1Aa** (1.0 equiv.), **2a** (1.2 equiv.), **Rh** (5 mol%), and CsOAc (2.0 equiv.) in TFE (*c* 0.2 M) at 23 °C for 20 h. Reactions were repeated twice and the results shown represent an average of both experiments. [b] Combined NMR yield of both diastereomers determined with an internal standard. [c] Determined by ^{1}H-NMR analysis of crude reaction mixtures.

B *with [Cp*RhCl$_2$]$_2$ (**Rh1**):*

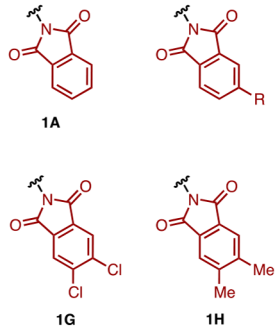

1A
1B R = F
1C R = Cl
1D R = Me
1E R = OMe
1F R = NO_2
1G
1H

entry[a]	phthalimide	% yield **3aa**[b]	*cis*/*trans* dr[c]
1	**1A**	69	31 : 69
2	**1B**	75	34 : 66
3	**1C**	68	36 : 64
4	**1D**	53	27 : 73
5	**1E**	58	32 : 68
6	**1F**	*47*	*51 : 49*
7	**1G**	72	44 : 56
8	**1H**	50	24 : 76

[a] Conditions: **1a** (1.0 equiv.), **2a** (1.2 equiv.), **Rh1** (5 mol%), and CsOAc (2.0 equiv.) in TFE (*c* 0.2 M) at 23 °C for 20 h. Reactions were repeated twice and the results shown represent an average of both experiments. [b] Combined NMR yield of both diastereomers determined with an internal standard. [c] Determined by ^{1}H-NMR analysis of crude reaction mixtures.

Figure 1. Optimization of the reaction conditions. (**A**) Evaluation of **Rh** catalysts with *N*-enoxyphthalimide **1Aa**. (**B**) Probing the impact of *N*-enoxyphthalimide electronics with catalyst **Rh1**.

formation of tri- and tetra-substituted cyclopropanes can be achieved routinely with very high diastereoselectivities using metal-catalyzed insertion of diazo reagents,[17] accessing 1,2-disubstituted cyclopropanes is less straightforward. Indeed, the majority of the developed methods afford their *trans*-diastereomers; access to the corresponding *cis*-congeners has remained elusive and relies on only a few available synthetic approaches.[18] Consequently, the finding of *cis*-diastereoselective reaction conditions would balance the existing methodologies and render the overall rhodium(III)-catalyzed cyclopropanation technology stereodivergent. Herein, we describe the implementation of this objective.

RESULTS AND DISCUSSION

Our efforts toward developing a *cis*-selective cyclopropanation reaction began by evaluating the influence of cyclopentadienyl ligands and *N*-enoxyphthalimides independently (Figure 1). First, 15 Cp^X-ligated rhodium(III) complexes (**Rh1**−**15**) were tested with the unsubstituted *N*-enoxyphthalimide **1Aa** as substrate and ethyl acrylate **2a** as its coupling partner (Figure 1A). Diastereoselectivity inversion occurs with increasingly encumbered Cp^X ligands, plateauing at a rather disappointing 64:36 diastereomer ratio with the bis-phenyl-Cp-ligated catalyst **Rh8** (Figure 1A, entry 8). In parallel, we also examined the impact of *N*-enoxyphthalimide electronics reasoning that while this change involves substrate engineering, *in situ* cleavage of the N−O bond renders it a traceless controller for the reaction. In the event, diastereoselectivity was modest among the various phthalimide groups tested, all of which favor the *trans*-cyclopropane diastereomer when used with the prototypical Cp*Rh(III) catalyst (**Rh1**), save the most electron-deficient **1F** which delivers the *cis*-adduct with a small preference of 51:49 dr (Figure 1B, entry 6).

We have recently reported a set of parameters for Cp^X ligands on rhodium(III) where the intricacies of steric and electronic effects are reduced to a collection of easily measured molecular descriptors.[19] These parameters have proven to be highly correlative in a number of multidimensional regression models. We envisioned that this approach would translate well to the development of a diastereodivergent cyclopropanation reaction, revealing the underlying physical organic parameters responsible for *cis*-selectivity, which may in turn be exploited to deliver a synthetically useful method.

With this idea in mind, we performed Sigman's multidimensional correlation analysis to gain additional information about the features of the catalyst that contribute to stereoselectivity (Figure 2).[20] A set of parameters for several Cp^X-ligated rhodium(III) complexes (**Rh**) was computed using the molecular models in Figure 2B. This parameter set includes IR vibrational frequencies (ν_S, an electronic descriptor), as well as Tolman cone angles (Θ_S) and Sterimol parameters (B_1 and B_5, steric descriptors) that we previously reported for a large number of piano-stool Cp^{X}Rh(III) complexes (see the Supporting Information). Given the preliminary results, *N*-enoxyphthalimides provided an additional leverage for perturbation. In order to describe the stereoelectronic features of these substrates, methoxyphthalimides were used as surrogates and their structures were computationally optimized at the B3LYP/6-311+G** level of theory[21,22] and the PBF solvation model for methanol.[23] From the optimized geometries, a number of electronic descriptors such as electrophilicity indicies, NBO charges,[24] IR frequencies, dipole moments, and polarizabilities[25] were enumerated (see Figure 2B and the Supporting Information).

With these descriptors in hand, we turned our attention to designing a data set in which both the **Rh** catalyst and phthalimide substrate are perturbed. To this end, 8 *N*-enoxyphthalimides **1A**−**H** and 12 rhodium(III) catalysts **Rh1**−**12** were selected and all possible permutations were evaluated under the reaction conditions. The resultant *cis*/*trans*-diastereomer ratios are presented in a color-coded matrix in Figure 2A. When taking a closer look at the **Rh1** column (prototypical Cp*Rh(III) catalyst), a slight increase in dr values is observed when moving from electron-rich (**1D**, $E_{1/2}^{Phth}$

DOI: 10.1021/jacs.8b04243
J. Am. Chem. Soc. XXXX, XXX, XXX−XXX

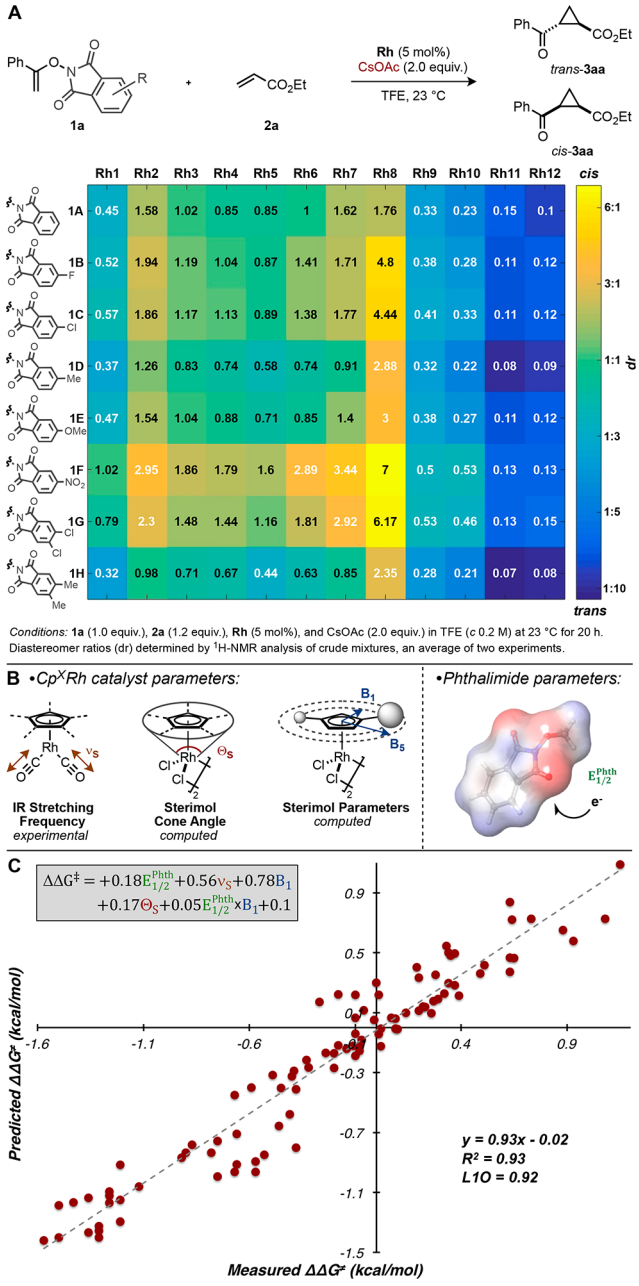

Figure 2. Optimization of reaction conditions by simultaneous variation of Rh catalyst and phthalimide structures with CsOAc base. (**A**) Heat-map of *cis*/*trans*-diastereomer ratios. (**B**) Models used for parametrization. (**C**) Correlation plot of normalized molecular descriptors to diastereomer ratios.

= −1.80 V, 27:73 dr; **1H**, $E_{1/2}^{Phth}$ = −1.86 V, 24:76 dr) to electron-deficient (**1F**, $E_{1/2}^{Phth}$ = −1.14 V, 51:49 dr; **1G**, $E_{1/2}^{Phth}$ = −1.52 V, 44:56 dr) phthalimide cores. Contrariwise, highly *trans*-diastereoselective reactions are seen (from 13:87 to 6:94 dr, blue color) when examining **Rh10**, **11**, and **12** columns that correspond to tetra-, tri-, and monosubstituted Cp^X rings, respectively. More synthetically useful *cis* selectivities are observed with other Cp^XRh(III)/phthalimide combinations (yellow-orange color), the two most selective catalyst/substrate pairs being the bis-phenyl-Cp complex **Rh8** with electron-deficient nitro- (**1F**) and dichloro-substituted (**1G**) phthalimides, delivering product in 88:12 and 86:14 dr, respectively. In addition to **Rh8**, a second region of high selectivity is located around the **Rh2**/**1F** and **Rh2**/**1G** coordinates (75:25 and 70:30 dr). Of note, the cyclohexyl-Cp-ligated complex (**Rh2**) and **Rh8** share comparably large cone angles (Θ_S = 187 and 191°, respectively), a feature that we anticipate to be important for high *cis*-diastereoinduction (*vide infra*).

The high variability of dr values across catalyst/substrate pairs is indicative of the magnitude of steric and electronic coupling between catalyst and substrate in the selectivity-imparting transition state (TS). One way to pinpoint such interactions is by performing a multivariate correlation analysis of our system.[26] Accordingly, when the acquired parameters are correlated with the measured dr values, expressed as $\Delta\Delta G^{\ddagger}$, the multidimensional model in Figure 2C is obtained that encompasses the entire catalyst−substrate data set (96 experimental outcomes). This model presents a good correlation (R^2 = 0.93, intercept = −0.02) and is statistically validated by the leave-one-out cross validation (L1O = 0.92). Four parameters appear in the equation: one phthalimide-based electronic descriptor, the redox potential ($E_{1/2}^{Phth}$), and three **Rh** catalyst-bound parameters, namely, the CO symmetric stretching frequency (ν_S), Sterimol B_1, and Sterimol cone angle (Θ_S) values.[27] As these are normalized models, the correlation coefficients denote the relative magnitude of each effect. While the Sterimol cone angle (Θ_S, normalized coefficient: +0.17) describes the overall isotropic volume of the Cp^X ligand, the larger coefficient (+0.78) of the Sterimol B_1 parameter underlines the importance of orientational effects. Additionally, an interaction cross-term appears between parameters $E_{1/2}^{Phth}$ and B_1. Although the coefficient is lower (+0.05), its inclusion improves the overall quality of the fit.[28] On the basis of some literature precedence that crossed terms signal direct noncovalent catalyst-substrate interaction,[25] we hypothesize that the electronic susceptibility of the phthalimide core to nucleophilic ring-opening (represented by $E_{1/2}^{Phth}$) and the accessible orientations of the Cp^X ring on the **Rh** catalyst (represented by B_1 and Θ_S) dictate the geometry of catalyst−substrate interaction at the selectivity-imparting TS. Highest selectivity sits on a saddle point between a sterically encumbered catalyst like **Rh8** (B_1 = 3.98 Å, Θ_S = 191°) or **Rh2** (B_1 = 3.96 Å, Θ_S = 187°) and an electron-deficient substrate like **1F** ($E_{1/2}^{Phth}$ = −1.14 V) or **1G** ($E_{1/2}^{Phth}$ = −1.52 V).

With the hypothesis that phthalimide ring-opening is required, we further examined the role of Lewis acidic additives on diastereoselectivity in the form of carboxylate base counterions. Several alkali metal acetates were surveyed;[29] the most drastic effect is seen when switching from CsOAc to NaOAc with a more than 2-fold increase in *cis*-diastereoselectivity (from 31:69 to 67:33 dr) for the prototypical **Rh1**/**1A** catalyst−substrate combination. Importantly, dr values rise significantly for most other catalyst/substrate pairs as well (color-coded matrix in Figure 3A). In search of a rationale of this unexpected counterion effect, we turned our efforts to establishing multivariate correlations for our 96-membered catalyst-substrate panel using NaOAc in place of CsOAc (Figure 3C).

It turned out that this new data set is sensibly less correlatable than the previously described CsOAc set and requires a minimum of five parameters for statistical robustness (R^2 = 0.90, L1O = 0.89). Phthalimides are now best described by μ_{B3LYP} (dipole moment) and $\alpha_{M06\text{-}2x}^{Phth}$ (mean polarizability); while **Rh** catalysts by ν_S, q_{Rh} (electronic) and B_1, Θ_S (steric) (Figure 3B). Closer inspection of the resultant correlation plot

DOI: 10.1021/jacs.8b04243
J. Am. Chem. Soc. XXXX, XXX, XXX−XXX

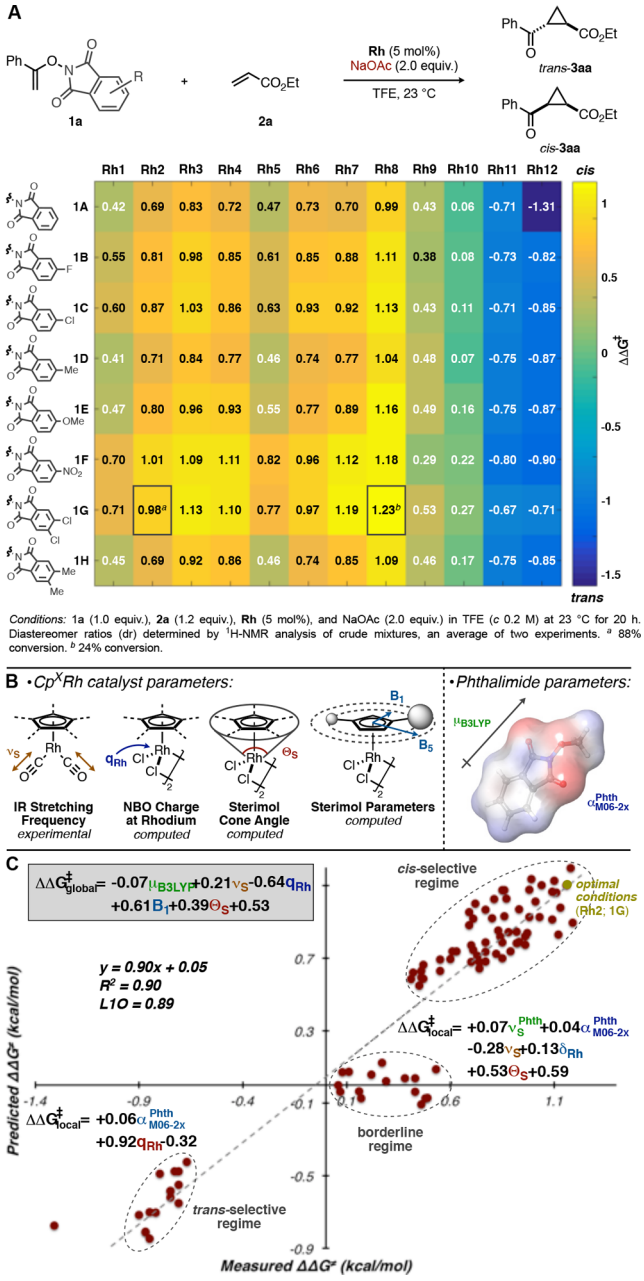

Conditions: 1a (1.0 equiv.), **2a** (1.2 equiv.), **Rh** (5 mol%), and NaOAc (2.0 equiv.) in TFE (*c* 0.2 M) at 23 °C for 20 h. Diastereomer ratios (dr) determined by ^{1}H-NMR analysis of crude mixtures, an average of two experiments. [a] 88% conversion. [b] 24% conversion.

Figure 3. Optimization of reaction conditions by simultaneous variation of Rh catalyst and phthalimide structures with NaOAc base. (**A**) Heat-map of *cis*/*trans*-diastereomer ratios. (**B**) Models used for parametrization. (**C**) Correlation plot of normalized molecular descriptors to diastereoselectivity (in the form of $\Delta\Delta G^{\ddagger}$ values).

exposes clustering of catalyst−substrate combinations in two regions according to their diastereoselectivity outcomes: (*i*) penta-substituted Cp^X ligands **Rh1**−**8** in combination with more electron-deficient phthalimides like **1B**, **1C**, and **1E-G** tend to bias the system toward phthalimide ring-opening resulting in higher *cis*-selectivity, whereas (ii) tetra-, tri-, and monosubstituted ligands **Rh10-12** lead to *trans*-selective reactions when used with more electron-rich phthalimides like **1A-E**, **1H**. The remaining permutations that include electronically and sterically mismatched catalyst-substrate pairs form a cluster displaying borderline selectivities that are poorly predicted by the parameter space (Figure 3C). The clustering behavior was scrutinized by splitting the entire data set in two subgroups, one for each *cis*- and *trans*-outcome, followed by building local correlation models, which displayed improved statistical performance (R^2 = 0.96 and 0.98; Q^2 = 0.93 and 0.95). Of note, while the *trans* local model is largely electronically driven (parameters $\alpha^{\text{Phth}}_{\text{M06-2x}}$ and $\mathbf{q}_{\text{Rh}}$), the *cis* local model has a large steric contribution (coefficient +0.53 in front of Θ_S). The appearance of correlative subgroups can be traced to the existence of two mechanistic regimes. While the mechanistic change is gradual with CsOAc and can be accounted for by the parameters space, this event is more abrupt with NaOAc and leads to clustering of correlations. The best-performing catalyst/substrate pairs are once again **Rh2**, **Rh8** in combination with **1F**, **1G**. Despite being slightly inferior to the **Rh8**/**1F** pair in terms of dr value, the cyclohexyl-Cp-ligated catalyst **Rh2** together with dichloro-substituted phthalimide **1G** gives higher isolated yield. Therefore, it was selected for further investigations.

The generality of our *cis*-cyclopropanation methodology was evaluated next with catalyst **Rh2**, NaOAc base, various 4,5-dichlorophthalimides **1G**, and alkenes **2** (Scheme 2).

Scheme 2. Generality of the cis-Cyclopropanation Reaction: (A) Optimized Conditions; (B) *N*-Enoxyphthalimide Scope; (C) Alkene Scope

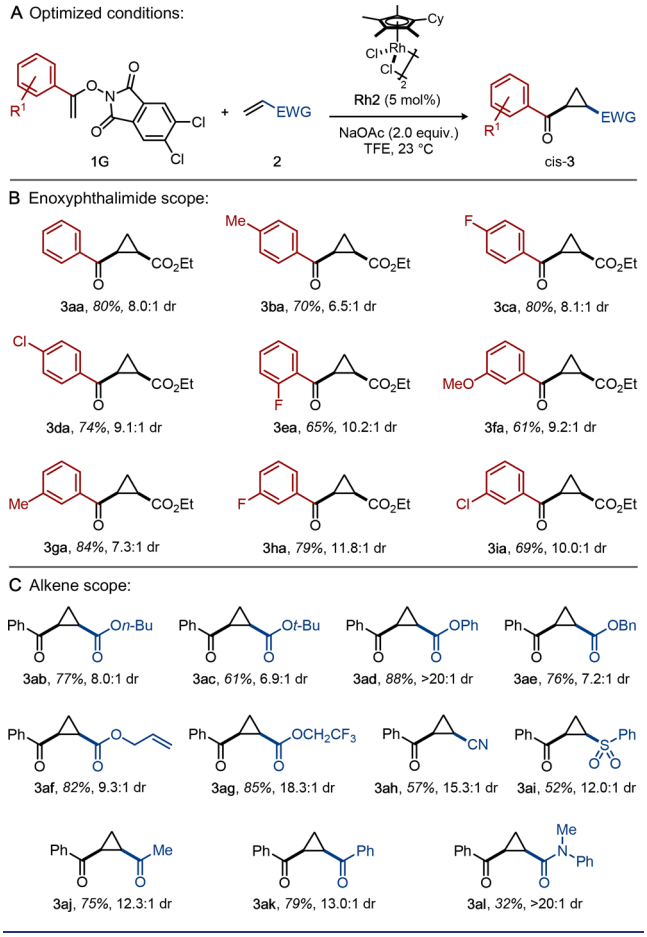

All reactions smoothly took place under mild conditions to furnish *cis*-cyclopropanes **3** in good yields (52−88%) and high diastereoselectivities (up to >20:1 dr). While electron-withdrawing substituents on the *N*-enoxyphthalimide rendered the cyclopropanation reaction more *cis*-selective (**3ca**, **3da**, **3fa**, **3ha**, and **3ia**), electron-donating groups provided slightly lower

DOI: 10.1021/jacs.8b04243
J. Am. Chem. Soc. XXXX, XXX, XXX−XXX

dr (**3ba** and **3ga**). The position of the substituents (*ortho*, *meta*, or *para*) is less critical for the efficiency of this transformation (**3ea**, **3ha**, and **3ca**). The reaction was compatible with versatile functional groups on the alkene component as representatively demonstrated by ester (**3ab**, **3ac**, **3ad**, **3ae**, and **3ag**), ketone (**3aj** and **3ak**), nitrile (**3ah**), sulfone (**3ai**), and amide (**3al**). In addition, the reaction is chemoselective and engages solely electron-deficient double bonds (**3af**).

Next, a series of deuterium labeling experiments were performed to interrogate the working model (Scheme 3).

Scheme 3. Proposed Mechanism: (A) KIE under *trans*-Selective Conditions; (B) KIE under *cis*-Selective Conditions; (C) Dichotomous Reaction Pathways

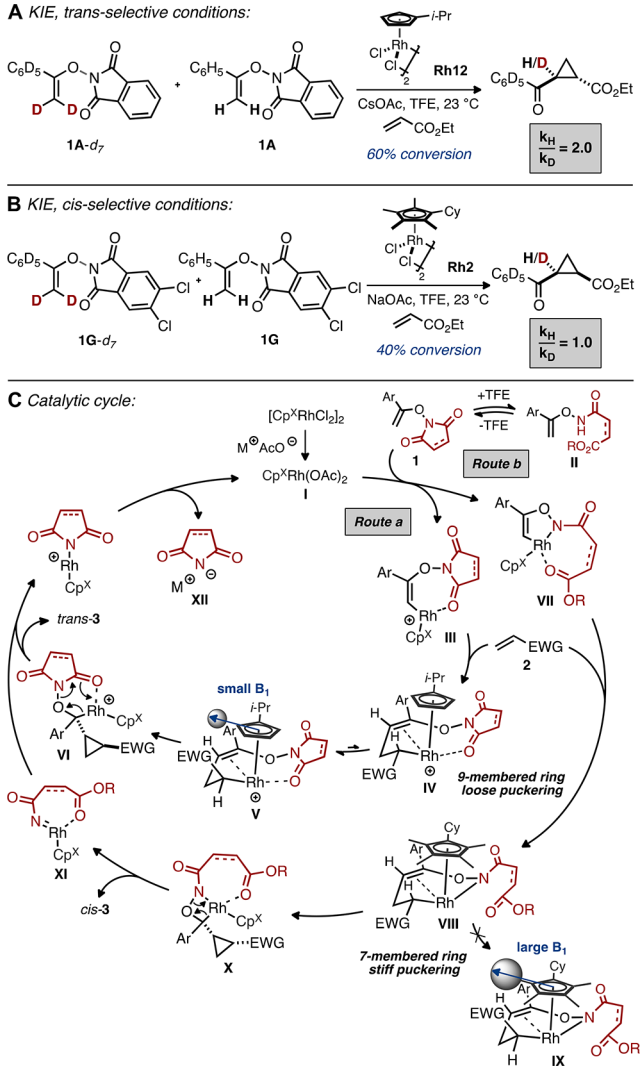

While a significant kinetic isotope effect (KIE) of 2.0 is seen under *trans*-selective cyclopropanation conditions (Scheme 3A),[13] no KIE is observed for the *cis*-cyclopropanation reaction (Scheme 3B), signaling that C−H activation is most probably not the rate-determining step for the latter. Taken together, these experimental results highlight the existence of a mechanistic dichotomy in pathways leading to *cis*- or *trans*-adducts, with a more electron-deficient phthalimide suggestive of an *in situ* ring-opening impacting diastereoselectivity. Additionally, *cis*−*trans*-isomerization experiments have shown that the dr values are under kinetic control under both the *trans*-[13] and *cis*-selective reaction conditions.[30]

Mechanistically, the crucial step is cleavage of the alkenyl C−H bond in **1** by *in situ* generated $Cp^XRh(III)$ acetato-complex **I** (Scheme 3C). To account for correlations and isotope labeling studies, we propose the occurrence of two parallel reaction routes: C−H activation can ensue either when directed by the intact phthalimide moiety (Route a) such as proposed for *trans*-cyclopropanation[13,31] or through a solvent-opened phthalimide ring **II** that acts as a bidentate ligand (Route b).[32] In the former case, C−H cleavage is rate-determining and consistent with the presence of a KIE, while in the latter case phthalimide ring-opening is presumably turnover-limiting and no KIE is expected. Next, the resultant seven- (**III**) or five-membered (**VII**) metalacycles undergo alkene **2** migratory insertion leading to ring-expanded cyclic intermediates **IV** or **VIII**, respectively, which are poised for a second (intramolecular) migratory insertion into the enolic carbon−carbon double bond that is selectivity-determining. The mechanistic rationale behind this hypothesis evokes rapid conformational equilibration of rhodacycles **IV** and **VIII** prior to the second migratory insertion step. Equilibrium position depends on the ring-size of the metalacyclic intermediate as well as the steric and electronic features of the phthalimide group and Cp^X ligand. In Route a, the small Sterimol $\mathbf{B_1}$ value of $Cp^{i\text{-}Pr}$ combined with conformationally flexible puckering of a 9-membered ring lessens steric clash between the pseudoaxial EWG group and Cp-ligand in conformer **V**, allowing formation of thermodynamically more stable *trans*-cyclopropane. Contrariwise, in Route b, a merger of the large Sterimol $\mathbf{B_1}$ of cyclohexyl-Cp with stiff puckering of a 7-membered ring leads to prohibitive steric interactions with the EWG in **IX**. In this case, the kinetic *cis* product is favored. The susceptibility of phthalimide to ring-opening and thus to engage in Route b is controlled by its electrophilicity, explaining the interplay between parameters $\mathbf{E}_{1/2}^{\mathbf{Phth}}$ and $\mathbf{B_1}$ in the correlation equation. Finally, the effect of base additive can be tentatively explained by the higher Lewis acidity of Na^+ versus Cs^+ cations leading to faster phthalimide ring-opening.

We assume that the coordinative interaction of the opened phthalimide ester group with rhodium(III) in intermediates **IV** and **VIII** is weakened due to presence of electron-withdrawing substituents on phthalimide that reduce the overall Lewis basicity of the carbonyl oxygens. While for **IV** this renders the 9-membered rhodacycle conformationally flexible and thus less sensitive to steric interaction between Cp^X and EWG, for **VIII** the remaining X-type ligation from the nitrogen atom of the opened phthalimide suffers less from the presence of electron-withdrawing substituents and maintains the stiffness of the 7-membered rhodacycle. This might explain the higher *cis*-selectivities that we observe with electron-deficient *N*-enoxyphthalimides. Additionally, the weakly coordinating ester side arm is outcompeted by the enolic carbon−carbon double bond that binds tightly to rhodium(III) in **VIII** favoring cyclopropanation over carboamination.

CONCLUSIONS

In summary, we have demonstrated that diastereoselectivity in $Cp^XRh(III)$-catalyzed cyclopropanation of alkenes using *N*-enoxyphthalimides can be switched from *trans* to *cis* by careful modulation of the stereoelectronic properties of substrate and catalyst. Guided by a 96-membered data set that was designed according to geometric, steric, and electronic criteria and used

DOI: 10.1021/jacs.8b04243
J. Am. Chem. Soc. XXXX, XXX, XXX−XXX

to construct quantitative structure−selectivity relationships, we promptly recognized that phthalimide ring-opening in conjunction with appropriate sterics of the Cp^X ligand on rhodium(III) play critical and synergistic roles in the diastereoselectivity-determining TS. Selectivity might be determined by the flexibility of rhodacycles **VIII** and **IV** derived from ring-opened versus -unopened phthalimides, respectively, induced by both their respective ring size (7- or 9-membered ring) and the Sterimol $\mathbf{B_1}$ parameter of the Cp^X ligand. The insights gained in the course of this study can be generalized to countless situations of catalyst-controlled selectivity, where multivariate regression analysis could supply a guided walk toward reaction optimization.

■ ASSOCIATED CONTENT

Supporting Information

The Supporting Information is available free of charge on the ACS Publications website at DOI: 10.1021/jacs.8b04243.

Supplementary text, additional Figures S1−S46, Tables S1 and S2, NMR spectra, computational details, statistical model development, and additional references 1−18 (PDF)

Parameters of complexes (XLSX)

Additional experimental data (XLSX)

■ AUTHOR INFORMATION

Corresponding Author

*tr2504@columbia.edu

ORCID

Fedor Romanov-Michailidis: 0000-0002-0997-478X

Tomislav Rovis: 0000-0001-6287-8669

Author Contributions

§T.P. and F.R.-M. contributed equally.

Author Contributions

⊥M.R.-M. and M.A.A. contributed equally.

Notes

The authors declare no competing financial interest.

■ ACKNOWLEDGMENTS

We gratefully acknowledge NIGMS (GM80442) for funding support.

■ REFERENCES

(1) (a) Bihani, M.; Zhao, J. C.-G. *Adv. Synth. Catal.* **2017**, *359*, 534−556. (b) Oliveira, M. T.; Luparia, M.; Audisio, D.; Maulide, N. *Angew. Chem., Int. Ed.* **2013**, *52*, 13149.

(2) Aggarwal, V. K.; Alonso, E.; Fang, G.; Ferrara, M.; Hynd, G.; Porcelloni, M. *Angew. Chem., Int. Ed.* **2001**, *40*, 1433.

(3) Deng, X.-M.; Cai, P.; Ye, S.; Sun, X.-L.; Liao, W.-W.; Li, K.; Tang, Y.; Wu, Y.-D.; Dai, L.-X. *J. Am. Chem. Soc.* **2006**, *128*, 9730.

(4) Johansson, C. C.; Bremeyer, N.; Ley, S. V.; Owen, D. R.; Smith, S. C.; Gaunt, M. J. *Angew. Chem., Int. Ed.* **2006**, *45*, 6024.

(5) Krautwald, S.; Carreira, E. M. *J. Am. Chem. Soc.* **2017**, *139*, 5627.

(6) Conway, J. H., Jr.; Rovis, T. *J. Am. Chem. Soc.* **2018**, *140*, 135.

(7) Wodrich, M. D.; Ye, B.; Gonthier, J. F.; Corminboeuf, C.; Cramer, N. *Chem. - Eur. J.* **2014**, *20*, 15409.

(8) Hong, S. Y.; Jeong, J.; Chang, S. *Angew. Chem., Int. Ed.* **2017**, *56*, 2408−2412.

(9) Ganesan, A. *Drug Discovery Today* **2002**, *7*, 47−55.

(10) Cernak, T.; Dykstra, K. D.; Tyagarajan, S.; Vachal, P.; Krska, S. W. *Chem. Soc. Rev.* **2016**, *45*, 546.

(11) For recent reviews, see: (a) Colby, D. A.; Bergman, R. G.; Ellman, J. A. *Chem. Rev.* **2010**, *110*, 624. (b) Satoh, T.; Miura, M. *Chem. - Eur. J.* **2010**, *16*, 11212. (c) Patureau, F. W.; Glorius, F. *Angew. Chem., Int. Ed.* **2011**, *50*, 1977. (d) Patureau, F. W.; Wencel-Delord, J.; Glorius, F. *Aldrichimica Acta* **2012**, *45*, 31. (e) Song, G.; Wang, F.; Li, X. *Chem. Soc. Rev.* **2012**, *41*, 3651. (f) Chiba, S. *Chem. Lett.* **2012**, *41*, 1554. (g) Piou, T.; Rovis, T. *Acc. Chem. Res.* **2018**, *51*, 170.

(12) For pioneering work, see: (a) Ueura, K.; Satoh, T.; Miura, M. *Org. Lett.* **2007**, *9*, 1407. (b) Umeda, N.; Tsurugi, H.; Satoh, T.; Miura, M. *Angew. Chem., Int. Ed.* **2008**, *47*, 4019. (c) Stuart, D. R.; Burgess, K. M. N.; Fagnou, K.; Bertrand-Laperle, M. *J. Am. Chem. Soc.* **2008**, *130*, 16474. (d) Fukutani, T.; Umeda, N.; Hirano, K.; Satoh, T.; Miura, M. *Chem. Commun.* **2009**, 5141. (e) Morimoto, K.; Hirano, K.; Satoh, T.; Miura, M. *Org. Lett.* **2010**, *12*, 2068. (f) Mochida, S.; Umeda, N.; Hirano, K.; Satoh, T.; Miura, M. *Chem. Lett.* **2010**, *39*, 744. (g) Hyster, T. K.; Rovis, T. *J. Am. Chem. Soc.* **2010**, *132*, 10565. (h) Rakshit, S.; Grohmann, C.; Besset, T.; Glorius, F. *J. Am. Chem. Soc.* **2011**, *133*, 2350.

(13) Piou, T.; Rovis, T. *J. Am. Chem. Soc.* **2014**, *136*, 11292.

(14) Ebner, C.; Carreira, E. M. *Chem. Rev.* **2017**, *117*, 11651.

(15) Evans, D. A.; Woerpel, K. A.; Hinman, M. M.; Faul, M. M. *J. Am. Chem. Soc.* **1991**, *113*, 726.

(16) Chen, Y.; Ruppel, J. V.; Zhang, X. P. *J. Am. Chem. Soc.* **2007**, *129*, 12074.

(17) (a) Chanthamath, S.; Takaki, S.; Shibatomi, K.; Iwasa, S. *Angew. Chem., Int. Ed.* **2013**, *52*, 5818. (b) Lindsay, V. N. G.; Nicolas, C.; Charette, A. B. *J. Am. Chem. Soc.* **2011**, *133*, 8972. (c) Rosenberg, M. L.; Vlašaná; Gupta, N. S.; Wragg, D.; Tilset, M. *J. Org. Chem.* **2011**, *76*, 2465. (d) Lindsay, V. N. G.; Lin, W.; Charette, A. B. *J. Am. Chem. Soc.* **2009**, *131*, 16383. (e) Nagashima, T.; Davies, H. M. L. *Org. Lett.* **2002**, *4*, 1989.

(18) (a) Suematsu, H.; Kanchiku, S.; Uchida, T.; Katsuki, T. *J. Am. Chem. Soc.* **2008**, *130*, 10327−10337. (b) Rosenberg, M. L.; Krivokapic, A.; Tilset, M. *Org. Lett.* **2009**, *11*, 547−550. (c) Brandenberg, O. F.; Prier, C. K.; Chen, K.; Knight, A. M.; Wu, Z.; Arnold, F. H. *ACS Catal.* **2018**, *8*, 2629. (d) Bachmann, S.; Furler, M.; Mezzetti, A. *Organometallics* **2001**, *20*, 2102. (e) Johansson, M. J.; Gorin, D. J.; Staben, S. T.; Toste, F. D. *J. Am. Chem. Soc.* **2005**, *127*, 18002. (f) Hu, W.; Timmons, D. J.; Doyle, M. P. *Org. Lett.* **2002**, *4*, 901.

(19) Piou, T.; Romanov-Michailidis, F.; Romanova-Michaelides, M.; Jackson, K. E.; Semakul, N.; Taggart, T. D.; Newell, B. S.; Rithner, C. D.; Paton, R. S.; Rovis, T. *J. Am. Chem. Soc.* **2017**, *139*, 1296.

(20) For a review, see Sigman, M. S.; Harper, K. C.; Bess, E. N.; Milo, A. *Acc. Chem. Res.* **2016**, *49*, 1292.

(21) (a) Stephens, P. J.; Devlin, F. J.; Chabalowski, C. F.; Frisch, M. J. *J. Phys. Chem.* **1994**, *98*, 11623. (b) Becke, A. D. *J. Chem. Phys.* **1993**, *98*, 5648. (c) Becke, A. D. *J. Chem. Phys.* **1993**, *98*, 1372. (d) Lee, C.; Yang, W.; Parr, R. G. *Phys. Rev. B: Condens. Matter Mater. Phys.* **1988**, *37*, 785.

(22) Krishnan, R.; Binkley, J. S.; Seeger, R.; Pople, J. A. *J. Chem. Phys.* **1980**, *72*, 650.

(23) (a) Tannor, D. J.; Marten, B.; Murphy, R.; Friesner, R. A.; Sitkoff, D.; Nicholls, A.; Ringnalda, M.; Goddard, W. A., III; Honig, B. *J. Am. Chem. Soc.* **1994**, *116*, 11875. (b) Marten, B.; Kim, K.; Cortis, C.; Friesner, R. A.; Murphy, R. B.; Ringnalda, M. N.; Sitkoff, D.; Honig, B. *J. Phys. Chem.* **1996**, *100*, 11775.

(24) Glendening, E. D.; Badenhoop, J. K.; Reed, A. E.; Carpenter, J. E.; Bohmann, J. A.; Morales, C. M.; Landis, C. R.; Weinhold, F. *NBO 6.0*; Theoretical Chemistry Institute, University of Wisconsin, Madison, WI, 2013.

(25) Polarizability ($\alpha^{\mathrm{Phth}}_{\mathrm{M06\text{-}2x}}$) single-point energy calculations were determined at the M06-2x/cc-PVTZ++ level of theory.

(26) Neel, A. J.; Milo, A.; Sigman, M. S.; Toste, F. D. *J. Am. Chem. Soc.* **2016**, *138*, 3863.

(27) In total, two series of regression equations were constructed, but only one is shown here because it benefits from better convergence and includes a phthalimide-bound parameter in addition to the catalyst ones. For a more detailed discussion on the building of correlations, see the Supporting Information.

DOI: 10.1021/jacs.8b04243
J. Am. Chem. Soc. XXXX, XXX, XXX−XXX

(28) Regression equations from the second series were also improved after inclusion of an interaction cross-term; see the Supporting Information.
(29) For KOAc, 51:49 dr is observed. For LiOAc, only trace amounts of the desired cyclopropane product are seen, presumably due to sparing solubility of LiOAc in TFE.
(30) An isomerization control experiment has been performed with two different catalysts, **Rh2** and **Rh8**: the dr values do not change as a function of reaction conversion, and the subjection of either diastereomer to the reaction conditions does not lead to any detectable isomerization; see the Supporting Information.
(31) For a discussion of alternative mechanistic interpretations in rhodium(III)-catalysis involving oxidizing directing groups, see Vasquez-Cespedes, S.; Wang, X.; Glorius, F. *ACS Catal.* **2018**, *8*, 242.
(32) Piou, T.; Rovis, T. *Nature* **2015**, *527*, 86.

DOI: 10.1021/jacs.8b04243
J. Am. Chem. Soc. XXXX, XXX, XXX−XXX